

Research Article

# MIG-seq is an effective method for high-throughput genotyping in wheat (*Triticum* spp.)

Kazusa Nishimura<sup>1</sup>, Ko Motoki<sup>1</sup>, Akira Yamazaki<sup>1,2</sup>, Rihito Takisawa<sup>3</sup>, Yasuo Yasui<sup>1</sup>, Takashi Kawai<sup>4</sup>, Koichiro Ushijima<sup>4</sup>, Ryohei Nakano<sup>1</sup>, and Tetsuya Nakazaki <sup>1\*</sup>

<sup>1</sup>Graduate School of Agriculture, Kyoto University, Kizugawa City, Kyoto Prefecture 619-0218, Japan, <sup>2</sup>Faculty of Agriculture, Kindai University, Nara City, Nara Prefecture 631-8505, Japan, <sup>3</sup>Faculty of Agriculture, Ryukoku University, Otsu City, Shiga Prefecture 520-2194, Japan, and <sup>4</sup>Graduate School of Environmental and Life Science, Okayama University, Okayama City, Okayama Prefecture 700-8530, Japan

\*To whom correspondence should be addressed. Tel. +81 0774 94 6404. Fax. +81 0774 94 6398.  
Email: nakazaki.tetsuya.4m@kyoto-u.ac.jp

Received 27 December 2021; Editorial decision 6 April 2022; Accepted 8 April 2022

## Abstract

MIG-seq (Multiplexed inter-simple sequence repeats genotyping by sequencing) has been developed as a low cost genotyping technology, although the number of polymorphisms obtained is assumed to be minimal, resulting in the low application of this technique to analyses of agricultural plants. We applied MIG-seq to 12 plant species that include various crops and investigated the relationship between genome size and the number of bases that can be stably sequenced. The genome size and the number of loci, which can be sequenced by MIG-seq, are positively correlated. This is due to the linkage between genome size and the number of simple sequence repeats (SSRs) through the genome. The applicability of MIG-seq to population structure analysis, linkage mapping, and quantitative trait loci (QTL) analysis in wheat, which has a relatively large genome, was further evaluated. The results of population structure analysis for tetraploid wheat showed the differences among collection sites and subspecies, which agreed with previous findings. Additionally, in wheat biparental mapping populations, over 3,000 SNPs/indels with low deficiency were detected using MIG-seq, and the QTL analysis was able to detect recognized flowering-related genes. These results revealed the effectiveness of MIG-seq for genomic analysis of agricultural plants with large genomes, including wheat.

**Key words:** MIG-seq, genotyping, wheat

## 1. Introduction

Detecting genome-wide genetic polymorphisms are essential for genetic analyses, such as linkage map construction and phylogenetic tree construction. For these genetic analyses, simple sequence repeats (SSR), restriction fragment length polymorphism, and cleaved amplified

polymorphic sequences markers have frequently been used. With the recent development of Next-Generation sequencing (NGS) technology, the cost of analysis for obtaining genotype data for molecular genetics has significantly reduced. In some crops, such as rice and soy, whole genome resequencing was applied for a genome-wide association study

(GWAS) with over 100 accessions.<sup>1,2</sup> Protocols, such as GBS (Genotyping by Sequencing) and RAD-Seq (Restriction Site-Associated DNA Sequencing),<sup>3,4</sup> which are restriction enzyme-based methods, have been developed. These methods are employed in several studies for genetic analyses because they reduce genome complexity and allow genotyping data to be obtained from large numbers of samples at a low cost. Afterward, double-digest RAD-Seq (ddRAD-seq), a method using two restriction enzymes, was reported.<sup>5</sup> Recently, Genotyping by Random Amplicon Sequencing-Direct (GRAS-Di) was developed as higher throughput genotyping by polymerase chain reaction (PCR) - based method,<sup>6</sup> and this technique was used for GWAS and linkage mapping in several crop species.<sup>7-10</sup>

Furthermore, NGS is useful for obtaining genomic polymorphisms for genomic analysis in wheat. At first, the genome of tetraploid wild species (*Triticum turgidum* L. ssp. *dicoccoides*) was sequenced and assembled, followed by the genome of a bread wheat (*Triticum aestivum* L. ssp. *aestivum*) cultivar, 'Chinese Spring', and the durum wheat genome (*T. turgidum* L. ssp. *durum*) were also assembled.<sup>11-13</sup> Recently, *de novo* assembly of several bread wheat varieties has been achieved.<sup>14</sup> However, it is still unreasonable to sequence the whole genome of more than 100 varieties for performing genetic analyses, such as GWAS, because the sequencing cost is too high for wheat. This is because wheat carries a large genome through allopolyploidization and duplication of many repetitive sequences, such as retrotransposons. Therefore, applying NGS analysis technologies with 'reduced complexity' for wheat and its relatives is effective, and several studies have been conducted using these methods.<sup>9,15,16</sup> Here, ddRAD-seq has been reported to be applied in many cases for genetic analysis of wheat, and this method is considered to be effective, but this method requires high-quality DNA, causing high cost for extraction and purification of DNAs. Therefore, the situation is such that further methodology improvement is expected.

Multiplexed inter-simple sequence repeats (ISSR) Genotyping by sequencing (MIG-seq), one of the 'reduced complexity' methods for building NGS libraries by PCR similar to GRAS-Di, was developed to analyze ecological studies.<sup>17</sup> With MIG-seq, libraries can be constructed in two PCR reactions: in the first PCR, the ISSR regions were amplified even from low-quality DNA, while in the second PCR, an index sequence for identifying individual samples was introduced. They reported that this method applies particularly to medium-scale studies based on less than 1,000 markers in ecology, phylogeography, and conservation genetics, including rapid studies of genetic differences among individuals (clones or varieties), populations, related species, and hybrids. However, as NGS analysis for linkage map construction is required to detect high-density single-nucleotide polymorphisms (SNPs), a MIG-seq is ineffective for genetic analysis, such as linkage mapping and GWAS. Consequently, MIG-seq has not been used for genetic analysis in major agricultural plant species so far, although this method has the advantage of not requiring high-quality DNA.

We hypothesized that MIG-seq might be useful for plant species with large genome sizes, such as wheat. There is a correlation between genome size and the number of SSRs in virus and mosquito species,<sup>18,19</sup> and we can expect that the number of loci that can be sequenced by MIG-seq will increase as the number of SSRs increases. Therefore, we can assume that sufficient polymorphisms can be detected in wheat with a large genome size. We conducted the following experiments to test this hypothesis. In this study, we demonstrated: (i) investigation of the relationship among the number of bases that can be sequenced stably by MIG-seq, genome size, and the

number of SSRs targeted by MIG-seq using 12 plant species that include various crops with diverse genome sizes, (ii) application of MIG-seq for population structure analysis, linkage map construction, and quantitative trait loci (QTL) analysis for heading date in tetraploid wheat to evaluate the effectiveness of MIG-seq for wheat.

## 2. Materials and methods

### 2.1. Plant materials

Four Tausch's goatgrass (*Aegilops tauschii* L.) accessions, four tetraploid and hexaploid wheat accessions each, four capsica (*Capsicum* spp.) accessions, two quinoa (*Chenopodium quinoa* L.) accessions, two strawberry (*Fragaria vesca* L.) accessions, four melon (*Cucumis melo* L.) accessions, four radish (*Raphanus sativus* L.) accessions, four cabbage (*Brassica oleracea* L.) accessions, four rose (*Rosa* spp.) accessions, four tomato (*Solanum lycopersicum* L.) accessions, and four peach (*Prunus persica* L.) accessions were used to evaluate MIG-seq performance for plant species with diverse genome size. These accessions were selected so that there would not be only varieties of the same clonal origin (e.g. bud sport mutant) within a species. [Supplementary Table S1](#) shows the information on these cultivars or accessions.

We used diverse tetraploid wheat collection (TWC) consisting of 195 pure accessions, including six subspecies: 55 domesticated emmer wheat (*T. turgidum* L. ssp. *dicoccum*), 114 durum wheat (*T. turgidum* L. ssp. *durum*), 10 Persian wheat (*T. turgidum* L. ssp. *carthricum*), 4 Colchis emmer wheat (*T. turgidum* L. ssp. *paleocolchicum*), 7 Polish wheat (*T. turgidum* L. ssp. *polonicum*), and 5 rivet wheat (*T. turgidum* L. ssp. *turgidum*) accessions for population structure analysis using SNP/indels obtained by MIG-seq ([Supplementary Table S2](#)). We used an F<sub>2</sub> tetraploid wheat population ( $n = 127$ ) and F<sub>6</sub> tetraploid wheat recombinant inbred lines (RILs) ( $n = 176$ ) for linkage map construction and QTL analysis ([Supplementary Table S3](#)). The F<sub>2</sub> population was derived from a cross between TTW41 (*T. turgidum* L. ssp. *dicoccum*: KU-3723) and TTW139 (*T. turgidum* L. ssp. *durum*: KU-3672). KU-3723 and KU-3672 are the accession numbers in NBRP KOMUGI (<https://shigen.nig.ac.jp/wheat/komugi/>). This F<sub>2</sub> population consisted of 127 individuals, 124 of which were used in Nishimura et al.<sup>20</sup> to analyze VRN-A3 (orthologous genes of *flowering locus T* in wheat<sup>21</sup>) effect on heading date. F<sub>6,7</sub> RILs were derived from a cross between TN26 (*T. turgidum* L. ssp. *dicoccum*) and TN28 (*T. turgidum* L. ssp. *durum*). F<sub>7</sub> progeny of F<sub>6</sub> RILs were used for investigating the heading dates under field conditions for QTL analysis.

### 2.2. Growth condition and heading data evaluation in wheat population

Eight F<sub>7</sub> seeds per line of RILs and 127 F<sub>2</sub> seeds were germinated on wet filter paper at 20°C under 24-h day length conditions on 5 November 2017 and 23 November 2017, respectively, and transplanted into 2 × 2 cell trays on 7 November 2017 and 26 November 2017. These plants were grown at 20°C in phytotron without artificial light, followed by transplantation into the experimental farm of the Graduate School of Agriculture, Kyoto University (34°44'02.4"N, 135°50'16.2"E) on 27 November 2017, and 7 December 2017. In each experimental plot, we planted seedlings at a spacing of 1 m between rows and 15 cm between individuals. Then, the heading dates of these segregation populations and used days from germination to heading (DGH) were recorded for QTL analysis.

### 2.3. MIG-seq library construction and NGS sequencing

Supplementary Table S1 shows the methods for extracting DNAs<sup>22</sup> for each accession of the 12 species. DNAs of TWC, the F<sub>2</sub> population and F<sub>6,7</sub> RILs were extracted from leaves of individuals using Dneasy Plant mini kit (Qiagen, USA), a method reported in Zheng *et al.*,<sup>23</sup> and Nucleon PhytoPure DNA extraction kit (GE Healthcare, Buckinghamshire, UK), respectively.

To evaluate the performance of MIG-seq, in the case of the experiment of first PCR of MIG-seq for the 12 species, the concentration of template DNAs to 20-ng/μl was adjusted using NanoDrop One (Thermo Fisher, Waltham, USA). Using 16 multiplexing primers developed by Suyama and Matsuki<sup>17</sup> (Supplementary Table S4) and Multiplex PCR Assay Kit ver.2 (TAKARA Bio Co. Ltd., Japan), the first PCR was performed using the following profile, referring to the method in Suyama *et al.*<sup>24</sup>: 94°C for 2 min, followed by 25 cycles at 94°C for 30 s, 38°C for 1 min, 72°C for 1 min, and a final extension at 72°C for 10 min. We performed the second PCR using Prime Star GXL DNA polymerase (TAKARA Bio Co. Ltd., Japan), the first PCR products diluted 50-fold, and the second PCR primers (Supplementary Table S5) with the following profile: 98°C for 30 s, followed by 20 cycles at 98°C for 10 s, 54°C for 15 s, 68°C for 30 s, and a final extension at 72°C for 10 min. Second PCR products of each sample in the same volume of liquid were pooled and purified using AMPure XP (Beckman Coulter, Inc., USA). The purified library was size-selected using SPRIselect (Beckman Coulter, Inc., USA). For removing fragments of small size (right side selection) and fragments of larger size (left side selection), the ratios of library sample to SPRIselect are 1:0.8 and 1:0.56, respectively. Of the 12 species, 151 bp paired-end reads of nine species except wheat and Tausch's goatgrass were obtained using the Illumina HiSeq X. The MIG-seq libraries of wheat and Tausch's goatgrass were sequenced using Illumina NovaSeq 6000, a pre-made library sequencing service (Novogene Co. Ltd, China), and obtained 150 bp paired-end reads of them.

To evaluate the relationship between the number of reads obtained and DNA concentration, the DNA of F<sub>6</sub> RILs and their parents were diluted 10-fold without checking the DNA concentration, and were used for the first PCR of MIG-seq. Then, the concentration was measured using Qubit<sup>TM</sup> dsDNA HS Assay Kit (Thermo Fisher Scientific, USA) after the first PCR. For the F<sub>2</sub> population of tetraploid wheat and TWC, the DNA concentration for MIG-seq library construction was not examined.

For TWC, we sequenced a dual-indexed library containing all samples (Supplementary Tables S2 and S5) using two lanes of HiSeq X, and 151 bp paired-end reads were obtained. In the case of the F<sub>6,7</sub> RILs, 192 sample libraries from 176 F<sub>6</sub> individuals and eight replicates of each of their parents were divided into four pooled libraries. Then, we added a unique dual index to 48 samples and pooled them into a single library (Supplementary Table S3). For these four pooled libraries, 150 bp paired-end reads were obtained using the Illumina NovaSeq 6000 pre-made library sequencing service. In the case of the F<sub>2</sub> population, all second PCR products (143 sample libraries from 127 F<sub>2</sub> individuals and eight replicates of each of their parents) were pooled with combinational dual indexes (Supplementary Tables S3 and S5), and 151 bp paired-end reads were obtained using the Illumina HiSeq X.

### 2.4. Bioinformatics pipeline

In the case of analysis for the 12 species, all data from the 151 bp paired-end sequence were trimmed to 150 bp paired-end data using

Trimmomatic v.2.0<sup>25</sup> with the following parameters, 'CROP : 150'. Because we derived the 17 bases at the 5' end of each raw read from the primer used in the first PCR of MIG-seq, all raw reads were trimmed and filtered using Trimmomatic v.2.0 with the following parameters, 'HEADCROP : 17 ILLUMINACLIP: TruSeq3-PE-2.fa : 2:30:10 LEADING : 20 TRAILING : 20 SLIDINGWINDOW : 4:15' (a FASTA format file, TruSeq3-PE-2.fa, contains Illumina adapter sequences, <https://github.com/timflutre/trimmomatic/blob/master/adapters/TruSeq3-PE-2.fa>). Using BWA mem,<sup>26</sup> we mapped the trimmed reads of the 12 species to reference genomes of each species (Supplementary Table S6)<sup>11–13,27–36</sup> after the sequence alignment/map (SAM) format files were converted to binary alignment map (BAM) and sorted using Samtools version 1.9.<sup>37</sup> In the case of an analysis to evaluate MIG-seq usefulness for various plant species, we used Samtools depth command to extract coverage depth (DP) information of each locus through genomes from sorted BAM with a set parameter, '-d 0'. In this study, nucleotides over 10 DP were defined as the number of sequences, which can be obtained stably by MIG-seq. The variant call is performed using the Samtools mpileup<sup>37</sup> command with the '-d 0' option. Raw reads of F<sub>2</sub> population, F<sub>6,7</sub> RILs, and TWC were filtered and mapped to the reference durum genome<sup>12</sup> in the same way, as stated above. For the variant calling of the TWC, F<sub>2</sub> population, and F<sub>6,7</sub> RILs, we used GATK Haplotype caller v4.1.7.0<sup>38</sup> to generate a 'g.vcf' format file for each sample. We performed joint genotyping using GATK GenomicsDBImport and GenotypeGVCF to create one VCF for each 'g.vcf' sample.

### 2.5. Investigating the number of bases that can be stably sequenced, extracting the number of SSRs, and nucleotide diversity in various plant species

For the analysis of the 12 species, the DP value was divided by the amount of raw read data (Gb) in each fastq file and multiplied by 0.5 to obtain the DP value per 0.5 Gb. Krait<sup>39</sup> was used to search the number of SSRs in the reference genome for the 12 species and summed the number of SSRs (ACT, TTG, GTG, and GT) appearing in the primers used for the first PCR of MIG-seq. We obtained the genome size from the number of bases in the FASTA file of the reference genomes and the correlation coefficients between the genome size and 'mapped base count', which is defined as the number of bases above DP 10. Then, we investigated the correlation between genome size and SSRs. Using VCFtools with the '-site-pi' option, we calculated the nucleotide diversity of each species.

### 2.6. Population structure analysis

After the bioinformatics process, we filtered the vcf file of TWC using VCFtools<sup>40</sup> with parameters: -max-missing 1 -minDP 5 -minQ 30 -recode -recode-INFO-all. To eliminate SNPs/indels containing heterozygous genotypes completely, the filter option of SnpSift was used with parameter: 'countHet()=0'. The filtered VCF was used for Admixture<sup>41</sup> to estimate individual ancestry. After PLINK 1.90<sup>42</sup> was used to remove SNPs in linkage disequilibrium with parameter: -make-bed -indep-pairwise 50 5 0.5 -allow-extra-chr, we ran Admixture. The phylogenetic tree of TWC was constructed using MEGA7<sup>43</sup> with SNPs obtained from MIG-seq. For principal component analysis (PCA), the VCF file was further filtered by PLINK 1.90 in linkage disequilibrium with parameter: -make-bed -indep-pairwise 50 10 0.1 -allow-extra-chr, and PCA was performed using PLINK 1.90.

## 2.7. Genetic linkage map construction and QTL analysis

The first VCF file was read by 'vcfR',<sup>44</sup> and genotypes with DP of 10 and DP of 5 or less were converted to missing data for the F<sub>2</sub> population and the F<sub>6:7</sub> RIL, respectively. Using handmade R script, individuals with extremely low genotype deficiency (less than 5% and 10% in the F<sub>2</sub> population and F<sub>6:7</sub> RILs, respectively) were deleted. For accurate linkage mapping, markers were filtered based on their genotype rate, the percentage of individuals whose genotype was obtained for a marker.

Linkage maps of the F<sub>2</sub> population and F<sub>6</sub> RILs were constructed using the R package 'one map'.<sup>45</sup> In the F<sub>2</sub> population, markers were grouped using the 'group' function of the 'Onemap' package, while in the case of F<sub>6:7</sub> RILs, markers were separated by chromosome and grouped using the 'group' function of 'Onemap' package. We calculated linkage distances using Kosambi's function (Kosambi 1944). The order of markers was determined using the 'order\_seq' function. QTL analysis was performed by the composite interval mapping (CIM) method using 'R/qrtl' package.<sup>46</sup> The threshold of the logarithm of odds (LOD) score was determined by the 1,000 permutation test.

## 2.8. Evaluating the accuracy of heterozygous genotype call

To investigate the amount of raw data and the minimum coverage depth that we can accurately call the heterozygous genotype data in the mapping population, the analysis was performed using the following procedures. First, the Seqkit<sup>47</sup> sample command was used to extract 0.5, 1.0, 1.5, 2.0, 2.5, and 3.0 million reads from eight replicates of TTW41 and TTW139 data, respectively. These sampled raw data of TTW41 and TTW139, respectively were independently merged to create eight independent replicates of virtual F<sub>1</sub> data. The amount of data in the virtual F<sub>1</sub> data is 1, 2, 3, 4, 5, and 6 million reads, respectively. For these data, VCF file was created using the same bioinformatics pipeline as the case of the F<sub>2</sub> population. Markers used to construct the linkage map of F<sub>2</sub> were extracted and the missing and error rates for each minimum coverage depth threshold (from 1 to 20) of the markers were calculated using handmade Rscript.

## 2.9. Calculation of nucleotide diversity of all combinations of two accessions in TWC

The number of polymorphisms (SNP/indels) between the two varieties was calculated for all combinations (18,721 combinations) of the TWC raw vcf file filtered by VCFtools<sup>40</sup> with parameters: `-minDP 5 -minQ 30 -recode -recode-INFO-all`. The number of SNPs was also calculated for the above vcfools condition with the `-remove-indels` option. The number of bases that could be sequenced with DP5 or higher was extracted using Samtools depth<sup>37</sup> command from BAM format files of TWC. Nucleotide diversity was calculated by dividing the number of SNPs between the two accessions by the number of bases with a DP of five or higher.

## 3. Results

### 3.1. Evaluation of MIG-seq performance for various plant species that include crop

We could obtain about 264,197,942 of 151 or 150 bp paired-end reads for the 12 species. Raw read counts for each sample ranged

from 3,482,874 (about 0.52 Gb) to 10,355,658 (about 1.55 Gb) (Supplementary Table S1). In this study, we investigated the relationship between the 'mapped base count', defined as the sum of the number of bases, with DP greater than or equal to 10, obtained from the whole genome, and the genome size calculated from the number of bases in the FASTA file for the 12 species. The results revealed that the mapped base count increased as the genome size increased, and that the common wheat, which has the largest genome size, had the largest mapped base count (Fig. 1A). Mapped base count and genome size were positively correlated ( $P$ -value  $< 2.2 \times 10^{-16}$ ,  $R = 0.986$ ) (Fig. 1A). To verify this result, we used Krait<sup>39</sup> to investigate the number of SSRs in the FASTA format files of the reference genomes of the 12 species because we expected the number of SSRs to increase with genome size and the number of ISSRs to increase accordingly. Using the results of SSR regions extracted from the reference genome of each species by Krait,<sup>39</sup> we calculated the total number of SSRs targeted by the primers used in the first PCR of MIG-seq. The number of SSRs was significantly associated with the genome size ( $P$ -value  $< 2.1 \times 10^{-13}$ ,  $R = 0.998$ , Fig. 1B). The SNPs detected by MIG-seq were distributed across the genome, but the DP values of each SNP/indel significantly varied among species. In wheat, the DP of several SNPs/indels was less than 1,000, but some polymorphisms exceeded 70,000 DP in radish (Fig. 1C, Supplementary Fig. S1). The nucleotide diversity of the 12 plant species ranged from 0.000825 to 0.0111. The rose materials used in this study had high nucleotide diversity, and we detected relatively many SNPs in the rose accessions (Supplementary Table S7).

### 3.2. Admixture analysis, constructing the phylogenetic tree, and PCA using SNP/indels from MIG-seq

We obtained 1,298,184,266 raw reads from two lanes of HiSeq X sequencing. Since the average number of raw reads per sample in TWC was 6,657,355.21, while the number of reads in TTW196 was 1,176,140, only the durum wheat line TTW196 was excluded from subsequent analyses (Supplementary Table S2). After filtering low-quality reads, mapping to the reference genome, and variant calling, we detected 3,848,416 SNP in the unfiltered VCF file. SNPs/indels with heterozygous genotypes and even a single missing data among accessions were removed, resulting in 8,207 polymorphisms (Table 1; 7,794 SNPs and 413 indel polymorphisms). We used 8,207 SNP/indels for PCA, while 7,794 SNPs were used for constructing phylogenetic trees by MEGA7. For Admixture analysis, 8,207 SNP/indels were filtered using PLINK 1.90, resulting in 4,947 SNP/indels (Supplementary Table S8).

Based on the results of the phylogenetic tree, hulled wheat was divided into four groups (EW1, EW2, CEW, and EW3) and free-threshing wheat was divided into four groups (PW, FTW1, FTW2, and FTW3) (Fig. 2A, Supplementary Figs S2 and S3). EW1, EW2, and EW3 were mainly composed of emmer wheat from USSR/Iran, Spain, and Ethiopia/India. CEW included all Colchis emmer wheat. For free-threshing wheat, PW includes Persian wheat. FTW1 was mainly composed of rivet wheat, durum wheat, and Polish wheat. FTW2 contained durum wheat derived from Egypt. Wheat accessions of FTW3 were durum wheat from various countries, and there seem to be several clades, but the bootstrap percentages for the first 10 branches of FTW3 were less than 30, so these were classified into one clade. Subspecies did not separate the PCA results, and some plots between subspecies were quite close and/or overlapped, but the same species tended to be located relatively close to each other (Fig. 2B). It was found that one sample of emmer wheat with large

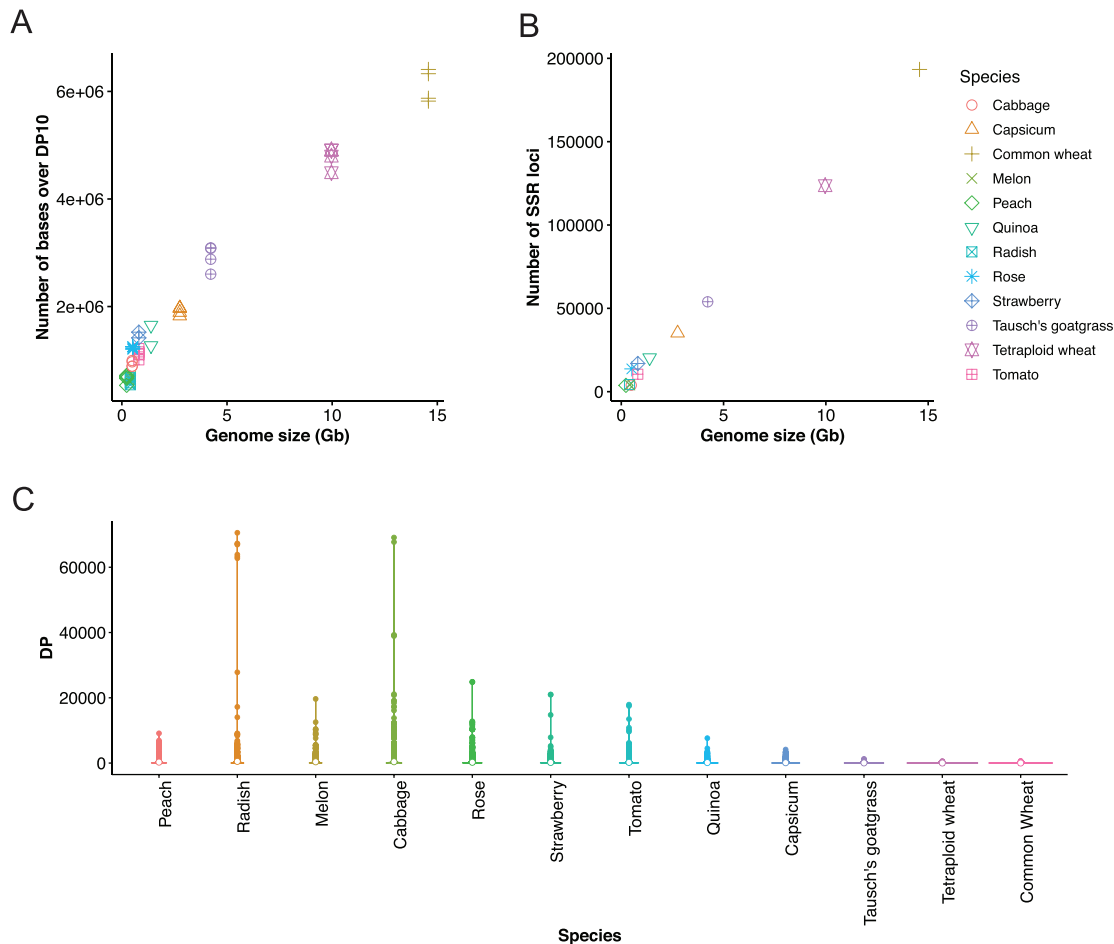


**Figure 1.** Evaluating the performance of MIG-seq using 12 plant species. (A) Relationship between genome size and the number of mapped base count. (B) Relationship between genome size and number of SSR loci number of SSRs present in the genome that are included in the primers of the first PCR of MIG-seq. (C) Violin plot of coverage depth (DP) of SNP/indel in each species. 'DP' is the average coverage depth for each polymorphism between/among accessions.

**Table 1.** Number of SNPs and indels of each chromosome in the  $F_2$  population,  $F_{6,7}$  RILs, and TWC

Chromosome	SNPs and indels in the $F_2$ population	SNPs and indels in the $F_{6,7}$ RILs	SNPs and indels in the TWC
1A	237	224	657
1B	238	227	427
2A	369	276	589
2B	334	313	524
3A	188	152	641
3B	262	304	667
4A	169	170	773
4B	157	246	577
5A	185	156	688
5B	168	223	510
6A	256	230	639
6B	241	234	403
7A	298	232	620
7B	155	197	532
All chromosome	3257	3148	8207

PC2 was TTW7 (KU-117), which is an accession that belongs to EW1 in the phylogenetic tree. This accession belongs to a different branch from the other 16 EW1 accessions (Supplementary Figs S2

and S3). As for admixture results, cross-validation revealed that the optimum  $k$  was 13 (Supplementary Fig. S4). The admixture results were broadly consistent with the phylogenetic tree results, although finer clades existed within EW2 and FTW3. In phylogenetic trees, durum wheat clades include rivet and Polish wheat, consistent with the previous study.<sup>12</sup> This finding supports the reliability of the polymorphism information obtained by MIG-seq.

### 3.3. Relationship between DNA concentration and amount of acquired data

Various DNA concentrations (from 0.291 ng/ $\mu$ l–56.0 ng/ $\mu$ l; Supplementary Table S3) of each line of  $F_{6,7}$  RILs were used for 1st PCR of MIG-seq. Then, we examined the relationship between the amount of DNA input and the number of raw reads obtained for each line used for linkage mapping. A weak positive correlation was observed between DNA concentration and number of raw reads for Library 1 and Library 3, but no significant positive correlation was observed for Library 2 and Library 4, suggesting that DNA concentration does not strongly affect the number of raw reads (Fig. 3). There was no positive correlation between the percentage of genotypes obtained in each individual of the  $F_6$  generation and DNA concentration used for the first PCR of MIG-seq (Supplementary Fig. S5).

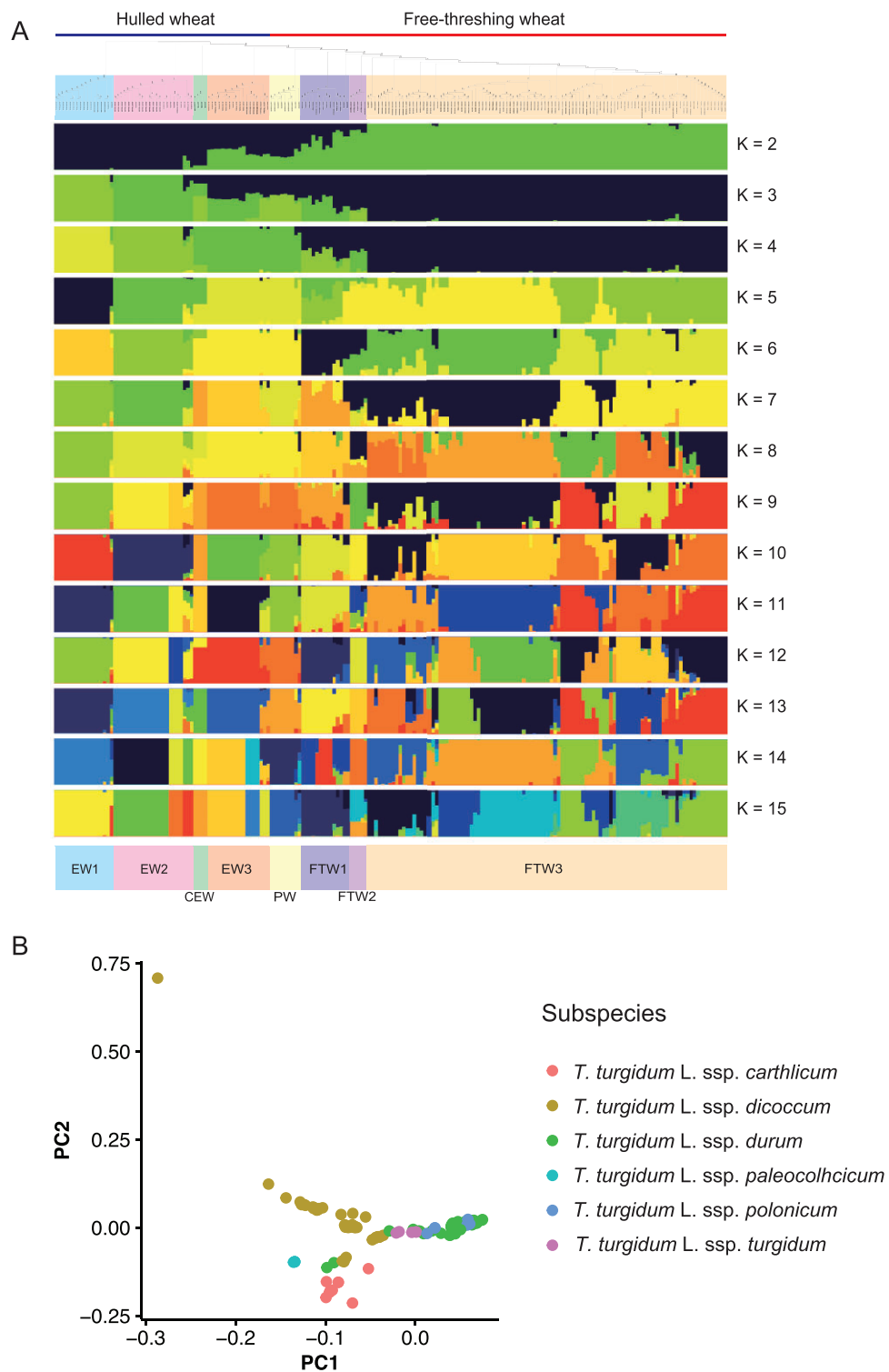


**Figure 2.** Admixture analysis, phylogenetic tree, and principal component analysis of tetraploid wheat population using SNP/indel markers obtained by MIG-seq. (A) Phylogenetic tree and admixture analyses in TWC. EW1, EW2, and EW3 consisted mainly of emmer wheat from the Soviet Union and Iran, Spain, Ethiopia, and India; CEW included all Colchis emmer wheat; EW2 included all emmer wheat from Egypt. PW includes Persian wheat. FTW1 consists mainly of rivet wheat, durum wheat, and Polish wheat. FTW2 contains durum wheat from Egypt. FTW3 contains durum wheat from various countries. (B) PCA of TWC using SNP derived from MIG-seq.

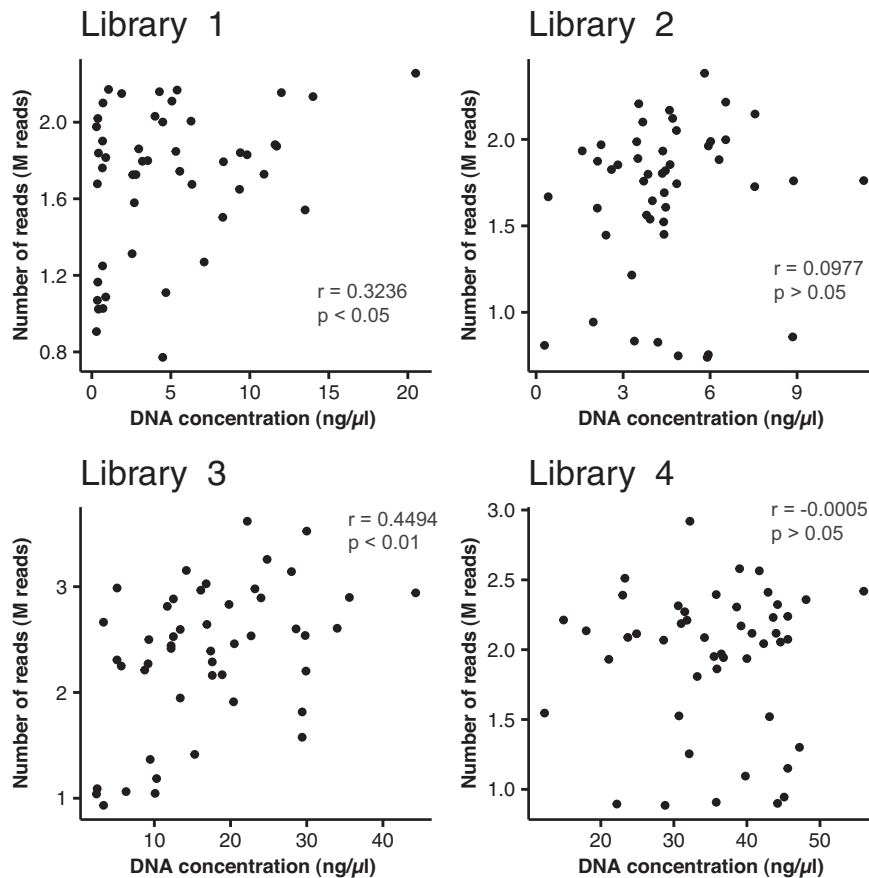


**Figure 3.** Scatter plot of DNA concentration vs. the number of reads obtained in  $F_{6:7}$  RILs. Library 1, Library 2, Library 3, and Library 4 indicate four independent MIG-seq libraries of  $F_{6:7}$  RILs consisting of 48 samples.

### 3.4. Linkage map construction of $F_2$ population and $F_{6:7}$ RILs

In the parental lines of  $F_2$  and  $F_{6:7}$  RILs, 43,110,852, 41,753,354, 8,298,912, and 15,331,396 raw reads were obtained for TTW41, TTW139, TN26, and TN28, respectively. The number of SNPs/indels between the parental lines that exhibited the same genotype and no missing values in eight replicates of the parental lines was 4,759 and 2,468 between the parental lines of the  $F_2$  population and the  $F_{6:7}$  RIL, respectively. The SNPs/indels that indicated the same genotype within the non-missing data and had polymorphisms between parental lines were 17,040 and 20,774 in  $F_2$  and  $F_{6:7}$ , respectively. In the case of merging data from eight iterations of the parent line, we detected 46,737 and 29,031 SNPs/indels between the parental lines of the  $F_2$  population (TTW41 and TTW139) and the parental lines of  $F_{6:7}$  RILs (TN26 and TN28), respectively.

We obtained 344,498,060 and 498,607,150 raw reads in  $F_2$  population and  $F_{6:7}$  RILs, respectively. Individuals with a high rate of missing genotype data in the segregating population were removed from subsequent analyses (data of one individual of the  $F_2$  population and one line of  $F_{6:7}$  RILs were removed). Considering the genotyping rate for markers (Supplementary Fig. S6), we extracted markers for which more than 97% of the individuals in the  $F_2$  population and more than 95% of the lines in the  $F_{6:7}$  population were genotyped. From these markers, 3,601 and 3,175 markers could be genotyped in the  $F_2$  population and  $F_{6:7}$  RILs, respectively. For  $F_{6:7}$  RILs, heterozygous genotype data were converted to missing data.

After grouping by OneMap ‘group’ function, we removed non-linked markers. We successfully generated a linkage map consisting of 3,257 and 3,148 markers in the  $F_2$  population and  $F_{6:7}$  RILs, respectively (Fig. 4, Table 1, Supplementary Figs S7–S9, Supplementary Data S1 and S2). The total length of the linkage map was 5,022.0 cM and 2,521.6 cM, and the average distance of loci was 1.54 cM and 0.80 cM in the  $F_2$  population and  $F_{6:7}$  RILs, respectively (Supplementary Tables S9 and S10). Comparing the genetic position and the physical position of the durum reference genome in both cases of linkage map in  $F_2$  population and  $F_{6:7}$  RILs, suppression of recombination near the centromere was observed, and the frequency of recombination increased near telomeres, as expected (Fig. 4). There were a few regions with few markers, such as 2A and 3A, but we obtained a map with marker information across the entire genome (Supplementary Fig. S10). For the  $F_{6:7}$  RILs, distortion of the segregation ratio was observed in the short arm of chromosome 5B (Supplementary Data S2).

### 3.5. QTL analysis for heading date

Figure 5 depicts the results of the QTL analysis. The DGH for the  $F_2$  population and  $F_{6:7}$  RILs ranged from 115 to 131 and from 157 to 180.5, respectively (Fig. 5A and B). The average DGH of TTW41, TTW139, TN26, and TN28 were 118.89, 126.80, 166.43, and 169.07, respectively. After 1,000 permutation tests, the LOD score thresholds were 6.09 and 5.09 for the  $F_2$

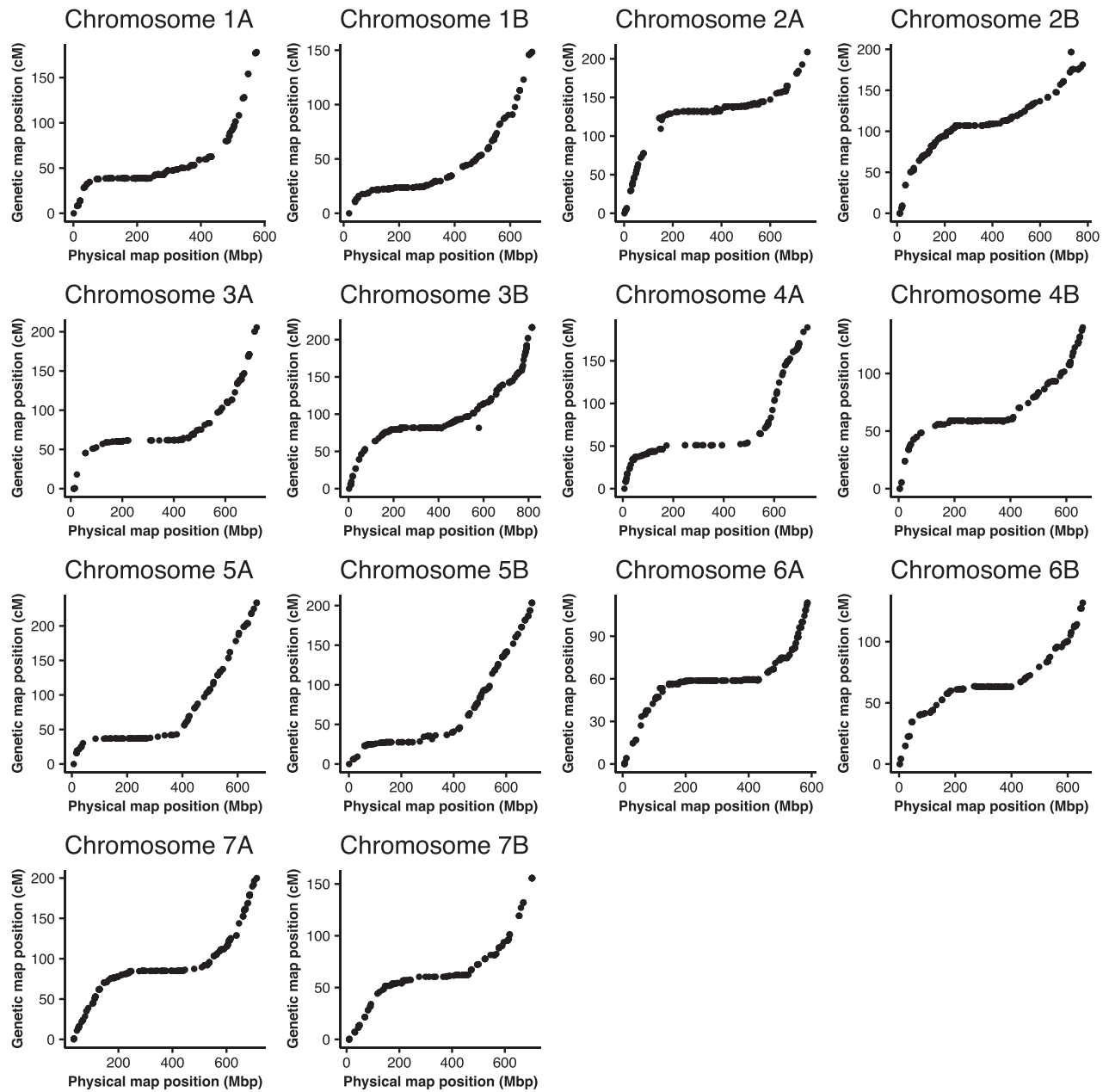


**Figure 4.** Dot plot of physical and genetic distances of markers on each chromosome for  $F_{6:7}$  RILs. The x-axis indicates physical map position of markers and the y-axis indicates genetic map positions of markers.

population and  $F_{6:7}$  RILs, respectively. In the  $F_{6:7}$  RILs, QTLs exceeding this threshold were detected on chromosomes 2A, 5A, and 7A, with LOD scores of 27.65, 5.35, and 22.78, respectively (Fig. 5C and D, Table 2). In the case of chromosome 2A QTL, the *Ppd-A1* gene<sup>48</sup> was located between the two markers (positioned between two markers: 2A\_36,075,870 and 2A\_41,495,996) flanking the peak of the LOD score. Similarly, the QTL of chromosome 7A and the QTL of chromosome 5A showed that the *VRN-A3*<sup>21,49</sup> (positioned between two markers: 7A\_68,283,463 and 7A\_76,232,738) and *Q* genes<sup>50</sup> (positioned between two markers: 5A\_604,404,784 and 5A\_622,238,335), which affect the time of heading and flowering, were located between the two markers that flank the peaks of LOD score. (Supplementary Fig. S11). The

similarity of the results of QTL analysis to SSR marker analysis in our previous study<sup>49</sup> indicates the accuracy of genotype data obtained by MIG-seq in wheat. In this study, a QTL at 7A chromosome was detected in this  $F_2$  population, as expected, since we assessed the effect of the *VRN-A3* gene on heading date using the same  $F_2$  population derived from a cross between TTW41 and TTW139 in our previous study.<sup>20</sup> The peak position of this QTL was not between the adjacent markers of *VRN-A3*.

### 3.6. Validating the amount of data for accurate heterozygous genotype calls

This study examined the amount of data and minimum DP threshold at which heterozygosity could be accurately estimated for the



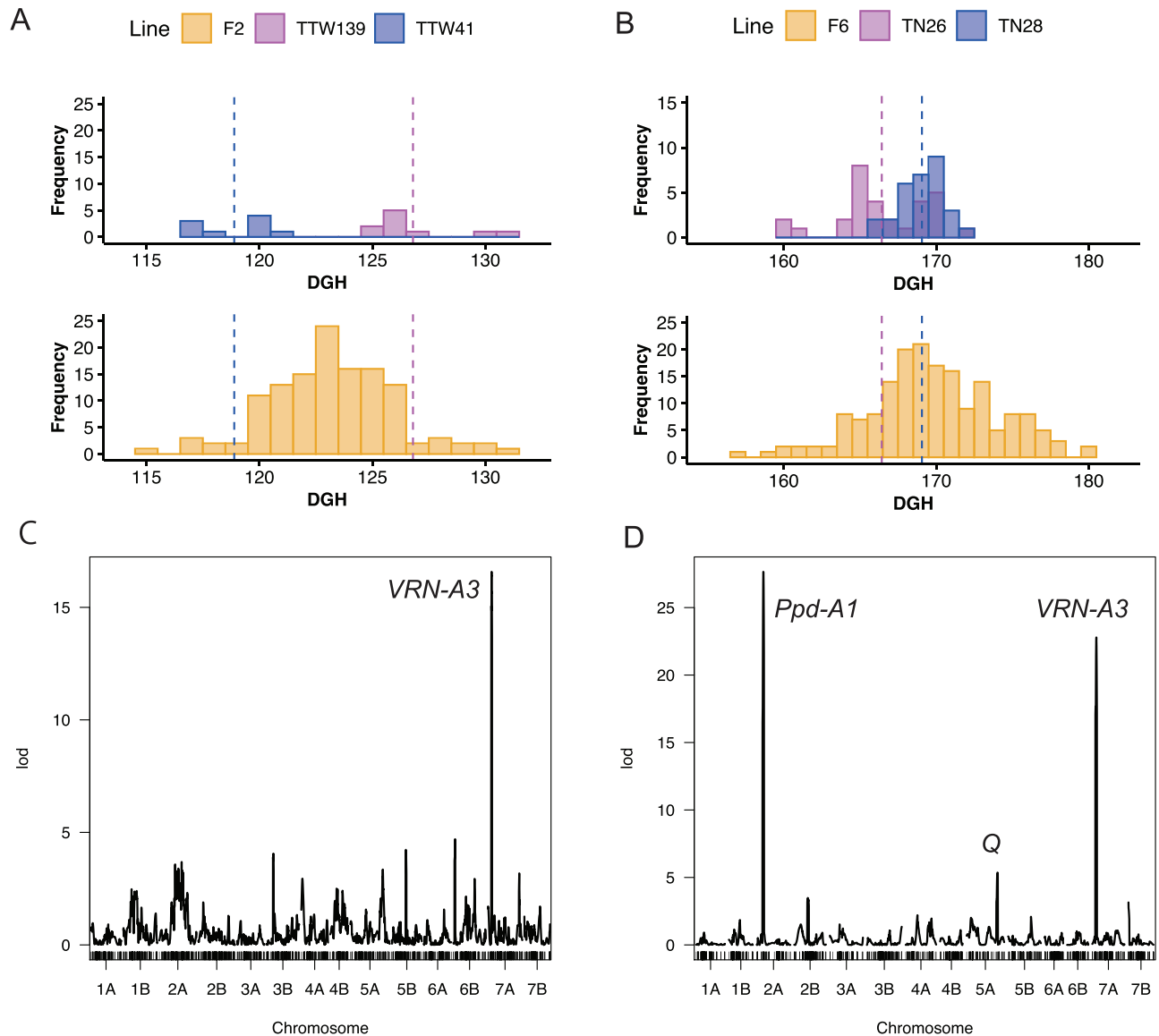


**Figure 5.** Phenotype data of F<sub>2</sub> population and F<sub>6,7</sub> RILs and their parents, and LOD scores of QTLs of F<sub>2</sub> population and F<sub>6,7</sub> RILs. (A) A histogram of DGH in the F<sub>2</sub> population and its parental lines. (B) A histogram of DGH in the F<sub>6,7</sub> RILs and its parental lines. Dotted lines mean the average DGH of two parental lines. (C) LOD scores of QTLs in the F<sub>2</sub> population. (D) LOD scores of QTLs in F<sub>6,7</sub> RILs.

markers used in F<sub>2</sub> linkage map construction. For 1 million reads, the error rate (the rate at which heterozygous loci are incorrectly identified as homozygous) was higher than for more than 2 million reads, and even with a minimum DP of 10, 4.58% of the data was in error (Fig. 6A). Increasing the minimum DP beyond 10 did not significantly improve the error rate. As the amount of data increased, the percentage of missing data reduced; for a minimum DP of 10, the percentage of missing data was less than 1% (0.24% missing) for more than 4 million reads (Fig. 6B). If about 4 million reads with a minimum DP of 10 or more was obtained, the heterozygous genotype with high accuracy could be expected. Alternatively, even with 6 million reads, the error rate did not reach zero, and no significant improvement of the error rate for 5 million reads was observed.

### 3.7. Distribution of nucleotide diversity between two accessions in TWC

To clarify the range of material wheat combinations for which a linkage map of > 1000 markers by MIG-seq is expected to be constructed, the distribution of the number of polymorphisms when using a collection of tetraploid wheat varieties was investigated. As the number of polymorphisms between two accessions is considered to be determined by the nucleotide diversity and number of common loci between the two accessions (number of bases with DP greater than 5 for both accessions), nucleotide diversity and common loci between the two accessions were calculated for all combinations selected from 194 varieties, two accessions at a time (18,721 combinations) (Fig. 7, Supplementary Figs S12 and S13 and Data S3). We found that the number of polymorphisms was strongly

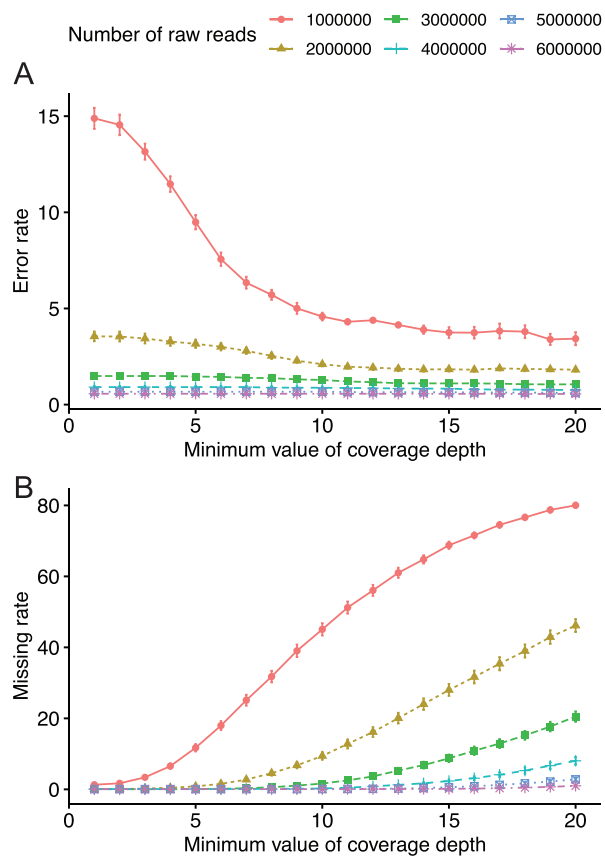


**Figure 6.** Assessing accuracy in calling heterozygous genotypes using data from virtual  $F_2$  between TTW41 and TTW139. (A) Genotyping error rate per minimum coverage depth and number of raw reads. The X-axis shows the minimum coverage depth required for genotype calling, and the Y-axis error rate shows the percentage of genotypes called as homozygous when they are called. The color line is changing depending on the amount of raw data. (B) Missing rate of genotypes per minimum coverage depth and number of raw reads.

correlated with nucleotide diversity in the present data set, while there was no positive correlation between the number of polymorphisms and the common loci between the two accessions (Supplementary Figs S13 and S14). On the other hand, a weak negative correlation was observed between nucleotide diversity and common loci between the two accessions (Supplementary Figs S13 and S14). As a result, we expect that the relationship between nucleotide diversity and the number of SNPs is not perfectly linear in the present data set. However, when data is extracted based on number of raw reads (mean number of raw reads between two accessions), the number of polymorphisms was almost linearly correlated to the nucleotide diversity (Supplementary Fig. S15). Therefore, by using a strong proportional relationship between nucleotide diversity and the number of SNPs in TWC, the number of markers that can be used to construct a linkage map between any two accessions as parents can be approximated from the number of markers of the linkage map constructed in this study and nucleotide diversity between the parental accessions, only for the data of TWC. The nucleotide diversity between TTW41 and TTW139 and that between TN26 and TN28 was 0.002548 and 0.002758, respectively. Then, assuming simple linearity between number of polymorphisms and nucleotide diversity, it

was predicted that a linkage map with over 1,000 markers could be created for accession combinations with a nucleotide diversity of at least 0.000782, which is the value of 1,000 divided by 3,257 (number of markers in linkage map of  $F_2$  population) multiplied by 0.002548 (the nucleotide diversity between TTW41 and TTW139), although it should be noted that not all polymorphisms between the parental accessions can be used as markers of low missing rate. The rate of combinations above this value (0.000782) was 82.76% between accessions in the same subspecies and 99.58% between accessions in different subspecies.

#### 4. Discussion

In this study, we applied MIG-seq to crops to detect polymorphisms for genetic analyses for the first time to the extent of our knowledge. From the results of evaluating the effectiveness of MIG-seq concerning genome size, we discovered that the number of bases that can be sequenced is associated with genome size. Additionally, the number of SSRs targeted by the first PCR of MIG-seq in the genome of species used in this study indicated a significant correlation with the genome size. Therefore, we have clarified that a relatively large number of loci could be sequenced by MIG-seq, and sufficient SNPs/indels could be obtained for genetic analysis in species with large genome sizes, such as wheat. Alternatively, we could not sequence more loci for plant species with a small genome size of less than a few Gb than species with a large genome. Although few polymorphisms may limit the accuracy of genetic analysis, the number of polymorphisms depends not only on the number of loci that can be sequenced but also on the genetic distance between accessions. Numerous polymorphisms could be obtained even in plant species with small genome sizes by MIG-seq using a sample with high nucleotide diversity ( $\pi > 0.01$ ), such as the rose used in this study.

When we examined the DP of each polymorphism obtained, we discovered a significant variation in the DP of each SNP/indels in species other than wheat. In some cases, we found regions with a DP of over 60,000 in radish and cabbage, which are too much DP for detecting polymorphisms (Fig. 1C, Supplementary Table S7). This variation may be attributed to the difference in amplification efficiency at each locus or amplification of repetitive sequences, such as retrotransposons, in the first PCR of a MIG-seq. Since over-sequencing the same locus more than 1,000 times is unlikely to improve the accuracy of genotype calling, the smaller the variation in the depth of each SNP, the more efficiently the genotype can be determined. Therefore, suppressing this variation by MIG-seq can result in more efficient detection of polymorphisms at a relatively low cost in any species other than wheat.

From the results of MIG-seq for  $F_{6:7}$  RILs, we showed that quantification of sample DNA is unnecessary to construct an NGS library by MIG-seq. In GBS and ddRAD-seq methods, the first step of library construction is restriction enzyme-based, which requires a certain amount of high-quality DNA, and thus either extraction method of high-quality DNA or the cost of DNA purification is required. In MIG-seq, the first reaction is a PCR, so the result is less affected by the quality of DNA. In this study, we could not evaluate the quality of DNA, but we succeeded in constructing a library using DNA obtained using a simple DNA extraction method without using phenol proposed by Zheng et al.<sup>23</sup> in the  $F_2$  population of tetraploid wheat. Also, in MIG-seq, we discovered that sequence data could be obtained if a certain amount of DNA could be input during the first PCR. Furthermore, we observed the amount of data did not increase

**Table 2.** QTLs for heading date in F<sub>2</sub> population and F<sub>6;7</sub> RILs using linkage map by MIG-seq

Population	Chromosome	Closest marker	Position (cM)	Peak position (cM)	LOD	Additive effect	R <sup>2</sup> (%)
F <sub>2</sub>	7A	7A_62760233	40.00–49.00	44.00	16.57	2.33	41.1
F <sub>6;7</sub>	2A	2A_36075870	36.00–45.00	41.00	27.65	−2.53	34.8
F <sub>6;7</sub>	5A	5A_604404784	190.00–194.00	192.00	5.35	0.96	7.0
F <sub>6;7</sub>	7A	7A_68283463	19.00–28.51	25.00	22.78	2.38	30.1

Plus values of additive effect mean the early flowering effect of TN26 allele in F<sub>6;7</sub> RILs, while that in F<sub>2</sub> population means the early flowering effect of TTW41 allele.

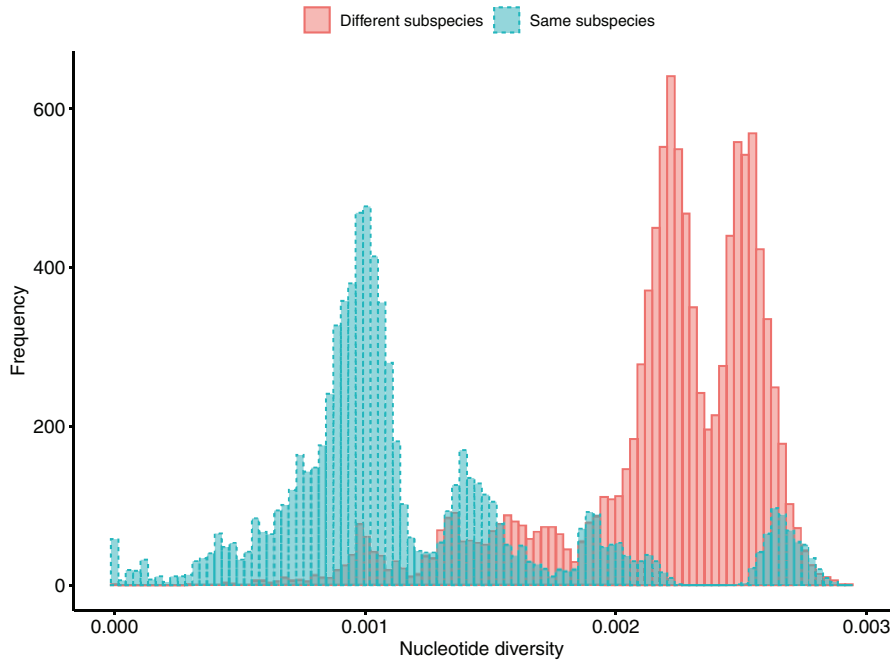


**Figure 7.** Bars surrounded by dashed line and solid line indicate nucleotide diversity between two accessions of same subspecies and that between two accessions of different subspecies, respectively.

proportionally with the DNA concentration. Therefore, we assumed that it is unnecessary to precisely normalize the DNA concentration using DNA-specific fluorescent dyes, although the lowest DNA concentration in this study was 0.291 ng per 7  $\mu$ l, at which the first PCR could be amplified, and it may need to be confirmed in the future whether the first PCR can be performed at lower concentrations. These results indicate that the main advantage of MIG-seq is that it eliminates the need for measurement and normalization of DNA concentration for each sample, thus saving cost and time for those experimental operations.

Our results indicated that the number of polymorphisms obtained by MIG-seq in wheat is equal to or slightly less than that of GBS methods reported in previous studies<sup>15,51,52</sup>. Although the wheat materials are different in each study, they reported that the numbers of GBS markers that could be genotyped in 80, 91.4, and 95% or more of the individuals were 8,505, 4,662, and 2,975, respectively. In contrast, in this study, we obtained 6,482 and 4,548 markers at 80 and 90% lines in F<sub>6;7</sub> RILs, and 6,609 and 4,866 markers at 80 and 90% individuals, respectively, in the F<sub>2</sub> population (Supplementary Fig. S6). The crosses used for constructing the

linkage map in this study were combinations of two lines with relatively high nucleotide diversity among TWC, and therefore, depending on the crossing combination, polymorphisms of 3,000 or more may not be obtained. Although the results of the calculation of the nucleotide diversity between the two cultivars indicated that the linkage map could be constructed with over 1,000 markers in most of the tetraploid wheat combinations (more than 82.76% for combinations between the same subspecies) it is necessary to verify the applicability of this method by studying the nucleotide diversity before constructing the linkage map. In the case of population structure analyses of TWC, we detected 8,207 SNP/indels with no missing genotypes. The number of polymorphisms detected in TWC is enough for population structure analysis. Considering the simplicity of DNA adjustment, we suppose that MIG-seq is a high-throughput method, which can be easily applied to larger populations, for example, to easily select core collections from populations of more than 1,000 individuals.

The genotype data from MIG-seq, like other NGS-based methods, may contain some error data. In the linkage map of Tausch's goatgrass generated by GRAS-Di, the number of markers in the linkage

map was significantly high but the total length of the genetic map was extremely longer than that constructed from non-GBS based markers<sup>53</sup>; over 800 cM for each chromosome.<sup>9</sup> It is reasonable to assume that this is not 800 cM, but error data. In this study, the linkage map was longer in the F<sub>2</sub> population than in the F<sub>6,7</sub> RILs, although the effect of having different parents in the F<sub>2</sub> population and the F<sub>6,7</sub> RILs had to be considered. This is because the F<sub>2</sub> population has more heterozygous loci than the F<sub>6,7</sub> RILs (Supplementary Fig. S8 and Data S1 and S2). If only reads from one parent chromosome were sequenced by chance, the locus would become homozygous, causing false double recombination. Double recombination, in which a heterozygote is inserted into a chromosomal region with a homozygous genotype was also observed (Supplementary Fig. S8 and Data S1 and S2). This could be due to sequencing errors, such as the false detection of fluorescence or index hopping in the sequencing step. In fact, in the hypothetical F<sub>1</sub> data generated using the F<sub>2</sub> parental line data, the error rate (error in which a genotype that should be heterozygous is determined to be homozygous) did not become zero even when the number of reads was increased to 6 million. Therefore, it is necessary to consider that a certain amount of error is always included in the analysis. In the case of QTL analysis, such as this study, a small amount of error data will not have a significant impact on the results of the analysis. However, more accurate genotype information may be required to determine the order of scaffolds in the *de novo* assembly of the genome. Since the cost of creating a library for MIG-seq is low, it is possible to increase the number of reads to be acquired and call genotypes or to sequence each strain multiple times and use only the data that match multiple times.

In this study, a clear distortion of the segregation ratio on chromosome 5B was also observed in the linkage map of F<sub>6,7</sub> RILs, which was also observed in our previous study (Nishimura et al.<sup>49</sup>), where the F<sub>5</sub> population derived from cross between TN26 and TN28 was genotyped using SSR markers (Supplementary Data S4). Therefore, it is not considered a bias caused by the MIG-seq method.

In this study, we discovered that genome size is associated with the number of bases that can be sequenced by MIG-seq, and as a result, a relatively large number of SNPs can be detected in wheat. Genotyping data with over 3,000 markers and a low defective rate could be obtained without precise normalization of DNA concentration between emmer wheat and durum wheat, and the possibility of constructing a linkage map of more than 1,000 markers with many tetraploid wheat combinations was shown. These results show that MIG-seq can be used for high-throughput genotyping of wheat.

## Acknowledgements

The National BioResource Project-Wheat with support in part from the National BioResource Project of MEXT, Japan provided almost all diploid wild wheat relative accessions, tetraploid wheat accessions, and hexaploid wheat accessions. A durum wheat cultivar, Setodur was provided by Western Region Agricultural Research Center, NARO. Two hexaploid wheat (Norin 61 and Chinese Spring), radish, and cabbage accessions were provided by NARO genebank ([https://www.gene.affrc.go.jp/index\\_j.php](https://www.gene.affrc.go.jp/index_j.php)). Melon accessions were provided by Dr. Kenji Kato (Okayama University). Dr. Mikihiro Yamamoto (Okayama University) provided strawberry accessions. Two quinoa accessions were obtained from the Germplasm Resources Information Network (GRIN) of the US Department of Agriculture (USDA). We deeply thank a team to cultivate field crops in Experimental Farm of Kyoto University (Chief, Mr. Hisashi Kagata) for supporting the cultivation of wheat. We also deeply thank Dr. Yoshiko Shimono for advice on the library construction of MIG-seq.

## Accession numbers

All sequence data obtained in this study were deposited to the DDBJ Sequence Read Archive under accession numbers, DRA013230, DRA013231, and DRA013232.

## Supplementary data

Supplementary data are available at DNARES online.

## Funding

This work was supported by a Grant-in-Aid for Early-Career Scientists (20K15502 to K.N.) from the Japan Society for the Promotion of Science.

## Author contribution

K.N. performed almost all of the experiments and analyses in this study. All authors discussed plant materials and extracted the DNA of each plant material. The first manuscript was written by K.N. and the other authors revised the manuscript. All authors checked the final manuscript.

## Conflict of interest

None declared.

## References

- Kajjiya-Kanegae, H., Nagasaki, H., Kaga, A., et al. 2021, Whole-genome sequence diversity and association analysis of 198 soybean accessions in mini-core collections, *DNA Res.*, **28**, dsaa032.
- Misra, G., Badoni, S., Anacleto, R., Graner, A., Alexandrov, N. and Sreenivasulu, N. 2017, Whole genome sequencing-based association study to unravel genetic architecture of cooked grain width and length traits in rice, *Sci. Rep.*, **7**, 12478.
- Baird, N.A., Etter, P.D., Atwood, T.S., et al. 2008, Rapid SNP discovery and genetic mapping using sequenced RAD markers, *PLoS One.*, **3**, e3376.
- Guo, Y., Yuan, H., Fang, D., et al. 2014, An improved 2b-RAD approach (I2b-RAD) offering genotyping tested by a rice (*Oryza sativa* L.) F<sub>2</sub> population, *BMC Genomics*, **15**, 1–13.
- Peterson, B.K., Weber, J.N., Kay, E.H., Fisher, H.S. and Hoekstra, H.E. 2012, Double digest RADseq: an inexpensive method for *de novo* SNP discovery and genotyping in model and non-model species, *PLoS One*, **7**, e37153.
- Enoki, H. and Takeuchi, Y. 2018, New genotyping technology, GRAS-Di, using next generation sequencer. In: *Proceedings of the Plant and Animal Genome Conference XXVI*, San Diego, CA.
- Kumawat, G. and Xu, D. 2021, A major and stable quantitative trait locus qSS2 for seed size and shape traits in a soybean RIL population, *Front. Genet.*, **12**, 646102.
- Moriya, S., Iwanami, H., Haji, T., et al. 2021, QTL analysis of crown gall disease resistance in apple: first plant R gene candidates effective against *Rhizobium rhizogenes* (Ti), *Tree Genet. Genomes*, **17**, 25.
- Miki, Y., Yoshida, K., Enoki, H., et al. 2020, GRAS-Di system facilitates high-density genetic map construction and QTL identification in recombinant inbred lines of the wheat progenitor *Aegilops tauschii*, *Sci. Rep.*, **10**, 1–12.
- Yoshikawa, S., Hamasaki, M., Kadomura, K., et al. 2021, Genetic dissection of a precocious phenotype in male tiger pufferfish (*Takifugu rubripes*) using genotyping by random amplicon sequencing, direct (GRAS-Di), *Mar. Biotechnol. (NY)*, **23**, 177–88.

11. Appels, R., Eversole, K., Feuillet, C., et al. 2018, Shifting the limits in wheat research and breeding using a fully annotated reference genome, *Science*, **361**, eaar7191.
12. Maccafferri, M., Harris, N.S., Twardziok, S.O., et al. 2019, Durum wheat genome highlights past domestication signatures and future improvement targets, *Nat. Genet.*, **51**, 885–95.
13. Avni, R., Nave, M., Barad, O., et al. 2017 Wild emmer genome architecture and diversity elucidate wheat evolution and domestication, *Science*, **357**, 93–97.
14. Walkowiak, S., Gao, L., Monat, C., et al. 2020, Multiple wheat genomes reveal global variation in modern breeding, *Nature*, **588**, 277–83.
15. Kobayashi, F., Tanaka, T., Kanamori, H., Wu, J., Katayose, Y. and Handa, H. 2016, Characterization of a mini core collection of Japanese wheat varieties using single-nucleotide polymorphisms generated by genotyping-by-sequencing, *Breed. Sci.*, **66**, 213–25.
16. Yang, Y., Dhakal, S., Chu, C., et al. 2020, Genome wide identification of QTL associated with yield and yield components in two popular wheat cultivars TAM 111 and TAM 112, *PLoS One*, **15**, e0237293.
17. Suyama, Y. and Matsuki, Y. 2015, MIG-seq: an effective PCR-based method for genome-wide single-nucleotide polymorphism genotyping using the next-generation sequencing platform, *Sci. Rep.*, **5**, 16963.
18. Zhao, X., Tian, Y., Yang, R., et al. 2012, Coevolution between simple sequence repeats (SSRs) and virus genome size, *BMC Genomics*, **13**, 435.
19. Wang, X.T., Zhang, Y.J., Qiao, L. and Chen, B. 2019, Comparative analyses of simple sequence repeats (SSRs) in 23 mosquito species genomes: identification, characterization and distribution (Diptera: Culicidae), *Insect Sci.*, **26**, 607–19.
20. Nishimura, K., Handa, H., Mori, N., Kawaura, K., Kitajima, A. and Nakazaki, T. 2021, Geographical distribution and adaptive variation of VRN-A3 alleles in worldwide polyploid wheat (*Triticum* spp.) species collection, *Planta*, **253**, 132.
21. Yan, L., Fu, D., Li, C., et al. 2006, The wheat and barley vernalization gene VRN3 is an orthologue of FT, *Proc. Natl. Acad. Sci. USA*, **103**, 19581–6.
22. Mizuno, N., Toyoshima, M., Fujita, M., et al. 2020, The genotype-dependent phenotypic landscape of quinoa in salt tolerance and key growth traits, *DNA Res.*, **27**, dsaa022.
23. Zheng, K., Subudhi, P.K., Domingo, J., Magpantay, G. and Huang, N. 1995, Rapid DNA isolation for marker assisted selection in rice breeding, *Rice Genet. Newsl.*, **12**, 48.
24. Suyama, Y., Hirota, S.K., Matsuo, A., et al. 2022, Complementary combination of multiplex high-throughput DNA sequencing for molecular phylogeny, *Ecol. Res.*, **37**, 171–81.
25. Bolger, A.M., Lohse, M. and Usadel, B. 2014, Trimmomatic: a flexible trimmer for Illumina sequence data, *Bioinformatics*, **30**, 2114–20.
26. Li, H. and Durbin, R. 2009, Fast and accurate short read alignment with Burrows–Wheeler transform, *Bioinformatics*, **25**, 1754–60.
27. Edger, P.P., Poorten, T.J., VanBuren, R., et al. 2019, Origin and evolution of the octoploid strawberry genome, *Nat. Genet.*, **51**, 541–7.
28. Jarvis, D.E., Ho, Y.S., Lightfoot, D.J., et al. 2017, The genome of *Chenopodium quinoa*, *Nature*, **542**, 307–12.
29. Parkin, I.A., Koh, C., Tang, H., et al. 2014, Transcriptome and methylome profiling reveals relics of genome dominance in the mesopolyploid *Brassica oleracea*, *Genome Biol.*, **15**, R77.
30. Luo, M.-C., Gu, Y.Q., Puiu, D., et al. 2017, Genome sequence of the progenitor of the wheat D genome *Aegilops tauschii*, *Nature*, **551**, 498–502.
31. Kitashiba, H., Li, F., Hirakawa, H., et al. 2014, Draft sequences of the radish (*Raphanus sativus* L.) genome, *DNA Res.*, **21**, 481–90.
32. Hosmani, P.S., Flores-Gonzalez, M., Geest van de, H., et al. 2019, An improved de novo assembly and annotation of the tomato reference genome using single-molecule sequencing, Hi-C proximity ligation and optical maps, *bioRxiv*, 767764. <https://doi.org/10.1101/767764>.
33. Raymond, O., Gouzy, J., Just, J., et al. 2018, The Rosa genome provides new insights into the domestication of modern roses, *Nat. Genet.*, **50**, 772–7.
34. Garcia-Mas, J., Benjak, A., Sanseverino, W., et al. 2012, The genome of melon (*Cucumis melo* L.), *Proc. Natl. Acad. Sci. U S A*, **109**, 11872–7.
35. Verde, I., Jenkins, J., Dondini, L., et al. 2017, The Peach v2.0 release: high-resolution linkage mapping and deep resequencing improve chromosome-scale assembly and contiguity, *BMC Genomics*, **18**, 225.
36. Kim, S., Park, M., Yeom, S.I., et al. 2014, Genome sequence of the hot pepper provides insights into the evolution of pungency in *Capsicum* species, *Nat. Genet.*, **46**, 270–8.
37. Li, H., Handsaker, B., Wysoker, A., et al.; 1000 Genome Project Data Processing Subgroup. 2009, The sequence alignment/map format and SAMtools, *Bioinformatics*, **25**, 2078–9.
38. McKenna, A., Hanna, M., Banks, E., et al. 2010, The genome analysis toolkit: a MapReduce framework for analyzing next-generation DNA sequencing data, *Genome Res.*, **20**, 1297–303.
39. Du, L., Zhang, C., Liu, Q., Zhang, X., Yue, B. and Hancock, J. 2018, Krait: an ultrafast tool for genome-wide survey of microsatellites and primer design, *Bioinformatics*, **34**, 681–3.
40. Danecek, P., Auton, A., Abecasis, G., et al.; 1000 Genomes Project Analysis Group. 2011, The variant call format and VCFtools, *Bioinformatics*, **27**, 2156–8.
41. Alexander, D.H. and Lange, K. 2011, Enhancements to the ADMIXTURE algorithm for individual ancestry estimation, *BMC Bioinformatics*, **12**, 246.
42. Chang, C.C., Chow, C.C., Tellier, L.C., Vattikuti, S., Purcell, S.M. and Lee, J.J. 2015, Second-generation PLINK: rising to the challenge of larger and richer datasets, *Gigascience*, **4**, 7.
43. Kumar, S., Stecher, G. and Tamura, K. 2016, MEGA7: molecular evolutionary genetics analysis version 7.0 for bigger datasets, *Mol. Biol. Evol.*, **33**, 1870–4.
44. Knaus, B.J. and Grünwald, N.J. 2017, vcfr: a package to manipulate and visualize variant call format data in R, *Mol. Ecol. Resour.*, **17**, 44–53.
45. Margarido, G.R.A., Souza, A.P. and Garcia, A.A.F. 2007, OneMap: software for genetic mapping in outcrossing species, *Hereditas*, **144**, 78–9.
46. Broman, K.W., Wu, H., Sen, S. and Churchill, G.A. 2003, R/qtl: QTL mapping in experimental crosses, *Bioinformatics*, **19**, 889–90.
47. Shen, W., Le, S., Li, Y. and Hu, F. 2016, SeqKit: a cross-platform and ultrafast toolkit for FASTA/Q file manipulation, *PLoS One*, **11**, e0163962.
48. Wilhelm, E.P., Turner, A.S. and Laurie, D.A. 2009, Photoperiod insensitive Ppd-A1a mutations in tetraploid wheat (*Triticum durum* Desf.), *Theor. Appl. Genet.*, **118**, 285–94.
49. Nishimura, K., Moriyama, R., Katsura, K., et al. 2018, The early flowering trait of an emmer wheat accession (*Triticum turgidum* L. ssp. *dicoccum*) is associated with the cis-element of the *Vrn-A3* locus, *Theor. Appl. Genet.*, **131**, 2037–53.
50. Simons, K.J., Fellers, J.P., Trick, H.N., et al. 2006, Molecular characterization of the major wheat domestication gene Q, *Genetics*, **172**, 547–55.
51. Brandt, K.M., Chen, X., Tabima, J.F., See, D.R., Vining, K.J. and Zemetra, R.S. 2021, QTL analysis of adult plant resistance to stripe rust in a winter wheat recombinant inbred population, *Plants (Basel)*, **10**, 1–22.
52. Hussain, W., Stephen Baenziger, P., Belamkar, V., et al. 2017, Genotyping-by-sequencing derived high-density linkage map and its application to QTL mapping of flag leaf traits in bread wheat, *Sci. Rep.*, **7**, 16394.
53. Boyko, E., Kalendar, R., Korzun, V., et al. 2002, A high-density cytogenetic map of the *Aegilops tauschii* genome incorporating retrotransposons and defense-related genes: insights into cereal chromosome structure and function, *Plant Mol. Biol.*, **48**, 767–90.